Identifying and characterizing regulators of histone acylation and replication stress

Kollenstart, L.

CHAPTER 4

The Mediator complex limits transcription-replication conflicts by preventing R-loop formation

Amandine Batté*, Leonie Kollenstart*, Mireille Tittel-Elmer, Su Ming Sun, Denise van Haren, Magdalena Miziołek and Haico van Attikum

* Equal contribution

ABSTRACT

In eukaryotic cells, DNA replication forks can encounter different types of DNA lesions or obstacles such as DNA-RNA hybrids (R-loops), which can cause replication fork stalling and/or collapse and consequently threaten genome stability. To properly deal with stalled or collapsed replication forks, cells have evolved a replication stress response, which regulates replication progression/recovery with cell cycle progression, transcription, and DNA repair. However, how this response is orchestrated and which proteins are involved is not yet fully understood. To fill this gap, we performed genome-wide screens to identify yeast mutants that are hypersensitive to hydroxyurea (HU), which induces replication stress by depleting dNTPs. We identified 285 mutants of known regulators in DNA replication and repair as well as several novel mutants. Subsequent scoring of Ddc2 foci, a well-established marker of replication stress, in the 80 most sensitive and novel mutants, revealed that several mutants in subunits of the Mediator complex, a well-conserved protein complex involved in transcription regulation, suffered from increased replication stress levels. Mediator mutants also experienced delayed replication fork progression and checkpoint activation. Importantly, we observed increased levels of R-loops in Mediator mutants. R-loops can be formed when transcripts are not properly targeted to the nucleopore complex (NPC), a process known as gene gating. Because of Mediators role in gene gating, we propose that Mediator prevents R-loop formation by promoting efficient gene gating, thereby preventing R-loop induced replication stress caused by replication-transcription conflicts.

INTRODUCTION

Faithful DNA replication is vital to prevent genome instability. However, replication forks can encounter various lesions or obstacles that can lead to replication fork stalling or collapse, collectively referred to as replication stress. For example, drugs like hydroxyurea (HU) cause replication fork stalling by depleting the pool of dNTPs. Alternatively, replication fork progression can also be blocked by obstacles such as interstrand crosslinks (ICLs), DNA adducts, G4-quadruplexes and the transcription machinery. Transcription blocks can lead to the formation of RNA-DNA hybrids (R-loops) which, in S-phase, can form a roadblock for the passage of the replication fork machinery. Particularly, when the transcription and replication machinery collide head-on, progression of the replisome is blocked, leading to replication fork stalling (Prado and Aguilera, 2005). A failure to stabilize and/or restart stalled replication forks can induce fork collapse, the formation of DNA double-strand breaks (DSBs) and, ultimately, genome instability. (González-Barrera et al., 2002).

Replication fork stalling through dNTP depletion by hydroxyurea (HU) has been extensively studied in *Saccharomyces cerevisiae.* Low levels of dNTPs impede replication fork progression, which results in stretches of single-stranded DNA (ssDNA) of around 200bp in length (Sogo et al., 2002). This ssDNA elicits a replication stress checkpoint that starts with coating the ssDNA with RPA complex (Rfa1-Rfa2-Rfa3). RPA contributes to the recruitment Mec1 (hATR) and its co-factor Ddc2 (hATRIP), leading to activation of Mec1 kinase activity and Mec1-dependent phosphorylation the Rad53 kinase (Rouse and Jackson, 2002; Zou and Elledge, 2003). Subsequently, Rad53 suppresses late origin firing, drives transcription of ribonucleotide reductase (RNR) genes, promotes cell cycle arrest, stabilizes stalled replication forks (Prado and Aguilera, 2005; Santocanale and Diffley, 1998; Tercero and Diffley, 2001; Zeman and Cimprich, 2014).

While many of the core factors involved in the response to replication stress have been identified and characterized, the entire plethora of proteins involved in regulating this complex response remains elusive. To increase our understanding of how cells prevent and deal with replication stress, we aimed to identify novel mutants in these processes by performing genome-wide HU sensitivity screens. In addition, we aimed to identifying HU-sensitive mutants that are unable to recover from replication stress by measuring Ddc2's accumulation into repair foci (Katou et al., 2003; Lisby et al., 2004). The HU sensitivity and Ddc2 foci screens identified over 40 mutants experiencing elevated levels of replication stress. Several of these mutants were members of the Mediator complex, which is a large multi-subunit protein complex that promotes the assembly of the preinitiation complex (PIC) and controls transcription (Soutourina, 2018).

While Mediator has been extensively described in various transcriptional processes, it is unclear how Mediator functions in replication stress. To understand how depletion of Mediator leads to increased replication stress, we performed several functional assays. Since Mediator did not locate to replication forks itself, but affects RNAPII occupancy in gene bodies, we investigated whether R-loops were formed due to deregulated transcriptional processes in the absence of Mediator. Indeed, R-loops are increased in Mediator mutants, leading to replication fork stalling. We hypothesize that Mediator limits replication stress by regulating RNAPII (un)loading or mRNA export. The latter prevents the back-hybridization of the nascent RNA with DNA, a process called gene gating (Gaillard et al., 2017; García-Benítez et al., 2017). Thus, our unbiased screening approaches revealed that Mediator prevents R-loop induced replication stress, likely by promoting gene gating.

RESULTS

Quantitative HU sensitivity screens identify Mediator and Clathrin complexes

To increase our understanding of how cells prevent and deal with replication stress, we performed quantitative high-throughput screens to identify yeast mutants that display increased sensitivity to HU. We robotically pinned the yeast haploid deletion collection consisting of ~5000 gene deletions of non-essential genes, and the Decreased Abundance by mRNA Perturbation (DAmP) collection, consisting of ~2000 strains containing hypomorphic alleles of essential yeast genes, in triplicate onto plates containing rich medium with or without 150 mM HU (Figure 1A). After 3-4 days of growth, colony sizes were measured using the previously established E-MAP tool (Bean et al., 2014). For each mutant, colony sizes in untreated and treated conditions were compared to reveal growth effects due to HU exposure (Figure 1A). Of the ~7000 mutants screened, we identified 283 yeast mutants to be HU sensitive (FDR <0.08 and colony size <20% decreased), while 202 appeared to be resistant to HU (FDR <0.08 and colony size <20% decreased) (Figure 1B). In the remainder of this chapter, we mainly focused on examining the mutants that displayed HU sensitivity. Of these mutants, 214 (75%) were from the gene deletion library and 71 (25%) were found in the DaMP collection. Importantly, 34 of the 285 sensitive mutants were in genes known to encode factors involved in the DNA damage response, including Rad54, Rad51, Pol32, Ino80, Pol ε and Orc3, showing the validity of the approach. One of the strongest hits was superoxide dismutase Sod1. Sod1 is important for the redox state of the cell and addition of the antioxidant NAC can suppress the HU sensitivity of Sod1 (Carter et al., 2005). Other hits were the 14-3-3 protein Bmh1, which affects the activity of checkpoint

kinase Rad53 (Usui and Petrini, 2007), and the motor proteins Kar3 and Cik1, which establish a kinetochore-microtubule interaction when centromeric DNA replication is slower (Liu et al., 2011; Liu et al., 2008). Interestingly, we also identified several mutants in genes not known to be linked to the replication stress response. These include *SOH1*, *SSN3* and *SRB2*, which encode components of the Mediator complex involved in transcriptional regulation (Jeronimo and Robert, 2017), and *SLA1*, *CHC1* and *CLC1*, which are involved in Clathrin-mediated endocytosis (Gardiner et al., 2007; Huang et al., 1997).

To validate findings from our screens, we first performed spot dilution tests for a subset of hits. For 6 out of 7 selected mutants we were able to confirm their HU sensitivity (Figure 1C). Next, we examined the overlap between hits from our screens and previously published HU sensitivity screens (Hartman and Tippery, 2004; Parsons et al., 2006; Woolstencroft et al., 2006). We found that out 99 of the 285 sensitive mutants in our screen had previously been identified. Specifically, 51, 91 and 27 hits overlap with those described by Parsons et al., Hartman et al., and Woolstencroft et al., respectively (Figure 1D). All studies used the same deletion library but applied different methods of quantification and different HU concentrations. Because of these variations, we applied the quantification method used in E-MAP screening (Bean et al., 2014), and generated our own dataset. Finally, to investigate our screen results in the context of gene-gene interactions, we performed a Spatial analysis of functional enrichment (SAFE) analysis. SAFE can annotate gene-gene or gene-drug interactions with gene ontology (GO) terms (Baryshnikova, 2018). This enabled us to assess the enrichment of our dataset in the 17 functional domains that map the genetic interaction similarity (GIS) network (Costanzo et al., 2016) (Figure 1E). The most enriched domain in the sensitive range was the "DNA replication & repair" cluster. The most enriched domain in the resistant range was the "respiration & mitochondrial oxidative phosphorylation" cluster. Since HU treatment increases ROS production, mutants in this cluster could decrease endogenous ROS production and therefore cause resistance, as is the case in *E. coli* (Nakayashiki and Mori, 2013). From these results, we conclude that our sensitivity screen was successful in identifying known as well as unknown factors that protect cells against HU-induced replication stress.

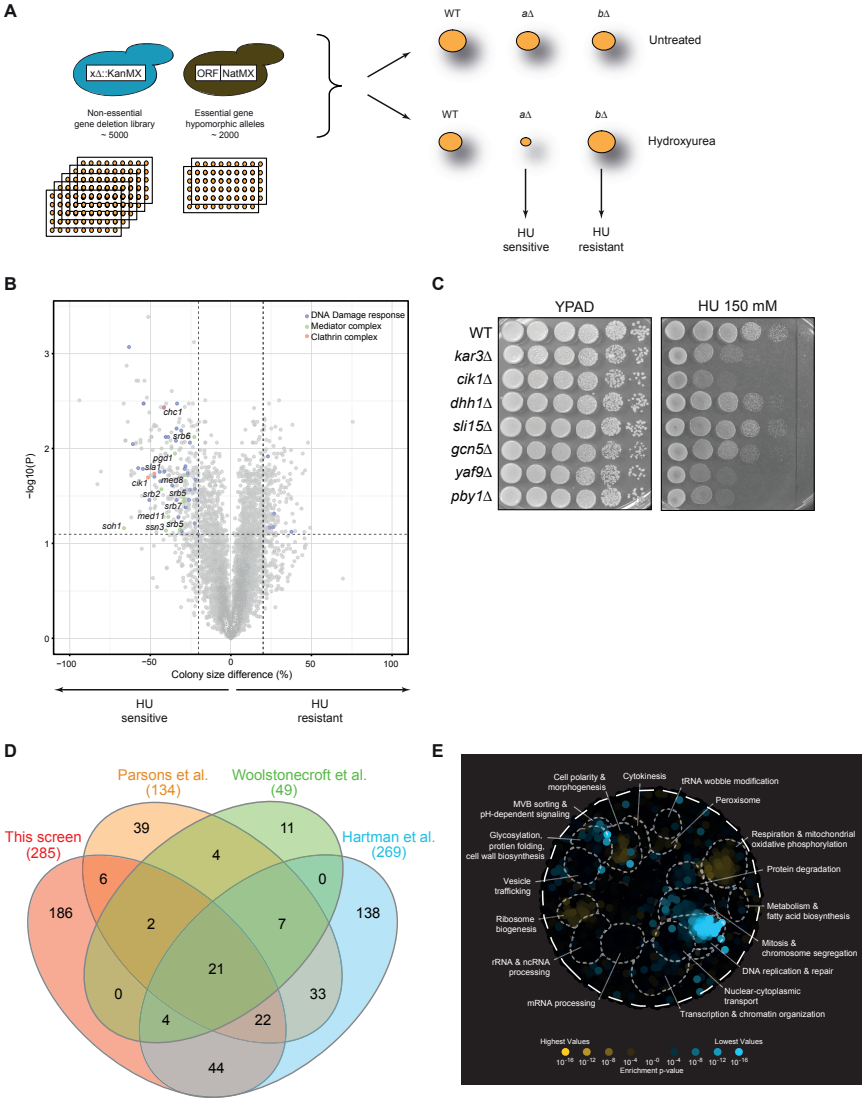

Figure 1. HU sensitivity screen identifies regulators the DNA damage response.
(A) Outline of colony growth screen. Knock-out and DaMP libraries of yeast mutants were plated on 1536 format and grown on plates containing rich media with or without 150 mM HU. Colonies with impaired growth under HU were considered sensitive and colonies whose growth was not affected by HU were considered resistant.
(B) Outcome of the sensitivity screen for approximately 7000 strains. Scatter plots show difference in colony growth in percentage versus their significance. Averages of three independent screens are shown and each dot represents a single mutant strain. DNA damage response factors are highlighted in blue and complexes selected for follow-up in green and red. (C) Spot dilution assay for a selection of hits from the screens. Cells were diluted and spotted on untreated plates and on plates containing 150 mM HU. (D) Venn diagram depicting the overlap between our screen and previously published HU screens. (E) SAFE analysis depicts enrichment of the HU screens in functional domains based on genetic interaction and GO enrichment data.

A focused Ddc2 foci screen reveals increased replication stress levels in Mediator and Clathrin complex mutants

When cells fail to recover from replication stress, the presence of RPA-coated ssDNA at stalled or collapsed forks will activate a checkpoint response by recruiting Mec1-Ddc2 to the ssDNA, the latter which can be monitored by the formation of Ddc2 foci (Lisby et al., 2004) (Figure 2A). To investigate whether the HU sensitivity observed for several top hits from our screens is a result of replication fork instability, we performed a focused Ddc2 foci screen. To this end, we counted Ddc2 foci after recovery from HU-induced stress in 82 of the 285 HU-sensitive mutants that have previously not been linked to replication stress. In addition, we included *rad52Δ* and *pol32Δ* as positive controls and *hoΔ* and *his3Δ* as negative controls. For this screen, mutants from the libraries were crossed with a strain expressing Ddc2-YFP. Out of 82 mutants, 45 mutants showed at least a 20% increase in Ddc2 foci formation, whereas 6 mutants showed a 15% decrease in Ddc2 foci formation (Figure 2A-B). The most striking hits were mutants in subunits of the Mediator (*soh1*, *srb2*, *srb5, med8, med11* and *ssn3*) and Clathrin (*chc1, clc1* and *sla1*) complexes, all of which showed elevated Ddc2 foci numbers. For these mutants, we validated results from the focused screen through independent Ddc2 foci formation experiments. Again, all mutants in subunits of Mediator and Clathrin showed more cells with Ddc2 foci as well as more foci per cell (Figure 2C-D).

Mediator is a large multi-subunit complex that is conserved across eukaryotes. It regulates transcription initiation together with RNA polymerase II (RNAPII) and several general transcription factors (Jeronimo and Robert, 2017). Mediator consists of four modules, the Head, Middle, Tail and cyclin kinase module (Figure 2E). The Middle module contains the most conserved Mediator subunits, among which is Soh1 (Med31) (Fan et al., 1996; Linder and Gustafsson, 2004)). This module is oriented toward RNAPII and is essential in yeast. The Tail and CDK8 kinase modules serve regulatory functions in transcription (Cevher et al., 2014; Plaschka et al., 2015). We found that mutants of head (*srb2*, *srb5*, *med8* and *med11*), middle (*med1 and soh1*) and kinase (*ssn3*) subunits of Mediator are sensitive to HU treatment and show elevated of Ddc2 foci levels, which is indicative of an increase in replication fork stalling/collapse (Figure 2E). Since loss of Mediator has not been linked to DNA replication stress, we chose to further investigate the role of this complex in preventing replication stress.

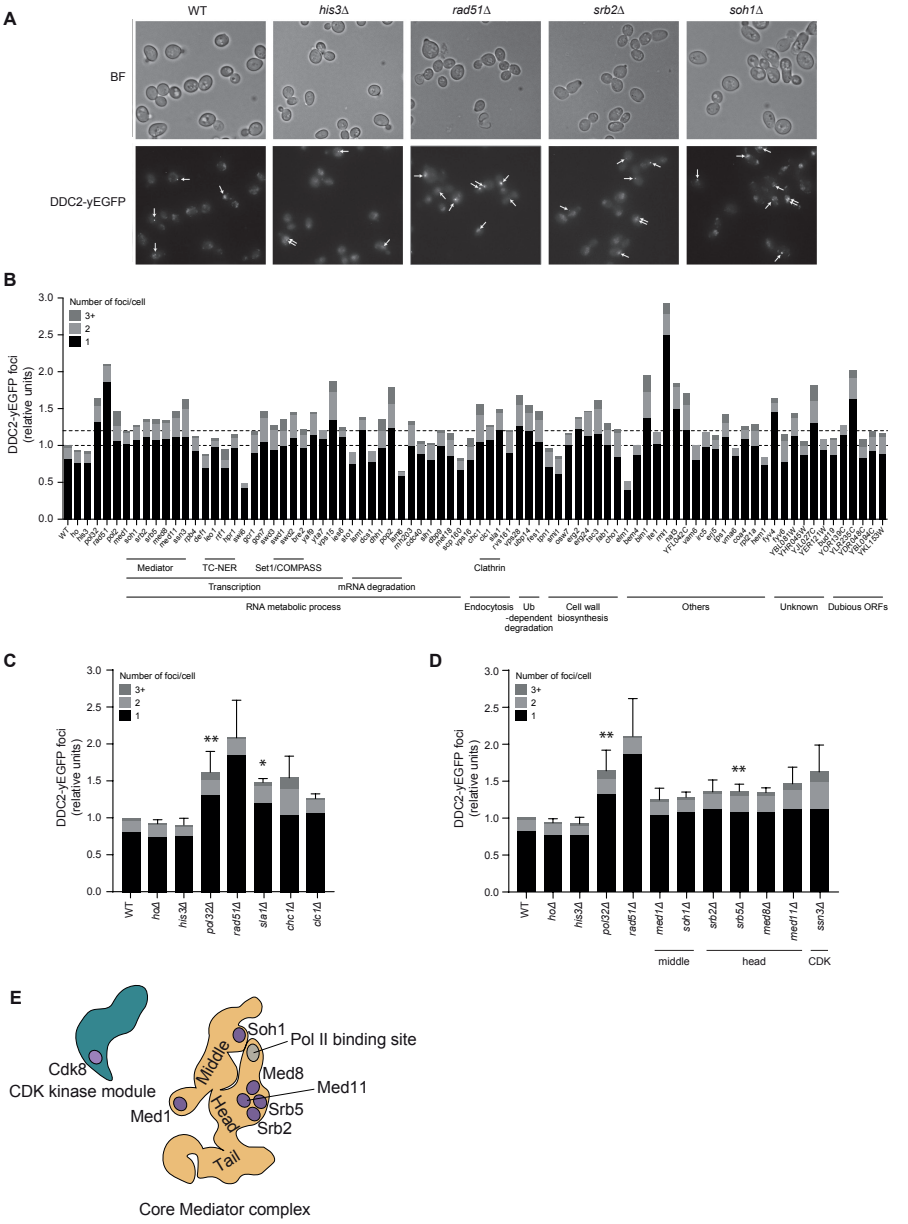

Figure 2. Ddc2 foci screen identifies increased replication stress in Mediator and Clathrin complex mutants.
(A) Ddc2 foci formation was scored after treating *his3Δ*, *rad51Δ, soh1Δ* and *srb2Δ* mutants with HU and letting them recover for 2 hours. Bright field and GFP channels are depicted. (B) Ddc2 foci scores for all tested mutants. (C) Ddc2 foci scores in Clathrin mutants. (D) Ddc2 foci scores in Mediator mutants. (C-D) Data are represented as the mean fold change from at least two independent experiments ± s.e.m. (E) Graphic representation of the Mediator complex. Subunits showing increased Ddc2 foci are highlighted.

Mediator mutants are sensitive to hydroxyurea and affect the progression of Pol epsilon

To examine a potential role for Mediator in the replication stress response, we first constructed mutants of *SOH1* and *SRB2 de novo* in a strain expressing Myc-tagged DNA Pol2, which we refer to as polymerase ε (Pol ε). We checked the growth of these two mutants on plates containing 50 mM and 100 mM HU. At both concentrations, loss of Soh1 or Srb2 sensitized cells to replication stress (Figure 3A), corroborating results from our HU sensitivity screens. To investigate whether loss of Mediator directly impacts replication fork integrity under stress conditions, we analyzed the progression of Pol ε at early-firing origin ARS607 and late-firing origin ARS501 (Figure 3B). After release of cells in S-phase in the presence of 0.2M HU, Pol ε is recruited to ARS607 in wild-type (WT) cells after 20 minutes and progresses along the chromosome arm after 40 and 60 minutes (Figure 3C). As expected, recruitment of Pol ε to late-firing ARS501 was not detectable at any of these timepoints. Interestingly, Pol ε recruitment to ARS607 was dramatically reduced in *soh1Δ* and *srb2Δ* when compared to WT at 20 minutes after release in HU, and became only fully recruited to ARS607 at 40 minutes, while showing progression into the surrounding chromatin after 60 minutes (Figure 3D-E). This suggests a delay in Pol ε progression under HU conditions in *soh1Δ* and *srb2Δ*.

To corroborate this delay in replication fork progression, we checked DNA replication through DNA copy number assays. After 40 minutes in HU, ARS607 was fully duplicated in WT cells with the +1 kb adjacent region reaching 2N after 60 minutes (Supplementary Figure 1A). Similar to Pol ε progression, DNA replication was delayed in Mediator mutants and full replication of ARS607 was only achieved after 60 minutes (Supplementary Figure 1B-C). This confirms that Mediator affects replication fork progression under replication stress conditions.

To determine whether the delay in replication fork progression is specific to replication stress conditions, we also investigated Pol ε recruitment near ARS607 in unstressed conditions at 20ºC, which allows slowing-down and capturing of the otherwise fast-moving replication forks. Pol ε recruitment to the origin of replication in wild-type cells started at 20 minutes and peaked at 30 minutes after release in S-phase (Supplementary Figure 1D). Similar to HU treated conditions, Pol ε accumulation was barely detectable after 20 minutes of release in S-phase and peaked only after 35 minutes in *soh1Δ* and *srb2Δ* when compared to WT (Supplementary Figure 1E-F), indicating that Mediator mutants also display delayed DNA replication in unperturbed conditions. We therefore conclude that Mediator promotes replication fork progression in unperturbed conditions and after HU-induced replication stress.

Mediator mutants display delayed S-phase entry and checkpoint activation

Since Pol ε recruitment is not decreased but rather delayed in the absence of Mediator, we investigated if this was linked to a delay in cell cycle progression and checkpoint activation. Therefore, we first determined the fraction of budded cells in WT and Mediator mutants as a read-out for S-phase entry (Zettel et al., 2003). Cells were synchronized in G1 with α-factor, released in rich medium containing 0.2M HU and sampled every 10 minutes for one hour. WT cells initiated budding at 20 minutes after release from G1 leading to 60% cells budding at 60 minutes after release in HU. In contrast, at 60 minutes less than 50% of s*oh1Δ* and *srb2Δ* cells contained a bud, suggesting that the progression into S-phase is delayed in the absence of Mediator (Figure 3F). Similar results were obtained when cells were released in S-phase in the absence of HU (Supplementary Figure 2A).

Next, we investigated the activation of the intra-S-checkpoint by stalled forks in Mediator mutants by monitoring the Rad53 phosphorylation status (Bjergbaek et al., 2005). Neither s*oh1Δ* and *srb2Δ* showed increase levels of spontaneous Rad53 phosphorylation (Figure 3G). In contrast, Rad53 activation was observed in WT cells following a 20-minutes exposure to HU. Both s*oh1Δ* and *srb2Δ* mutants were able to activate Rad53, but only after 40 minutes (Figure 3G). Thus, loss of Mediator delays both DNA replication and activation of the intra-S-phase checkpoint following HU exposure, likely by a delayed S-phase entry.

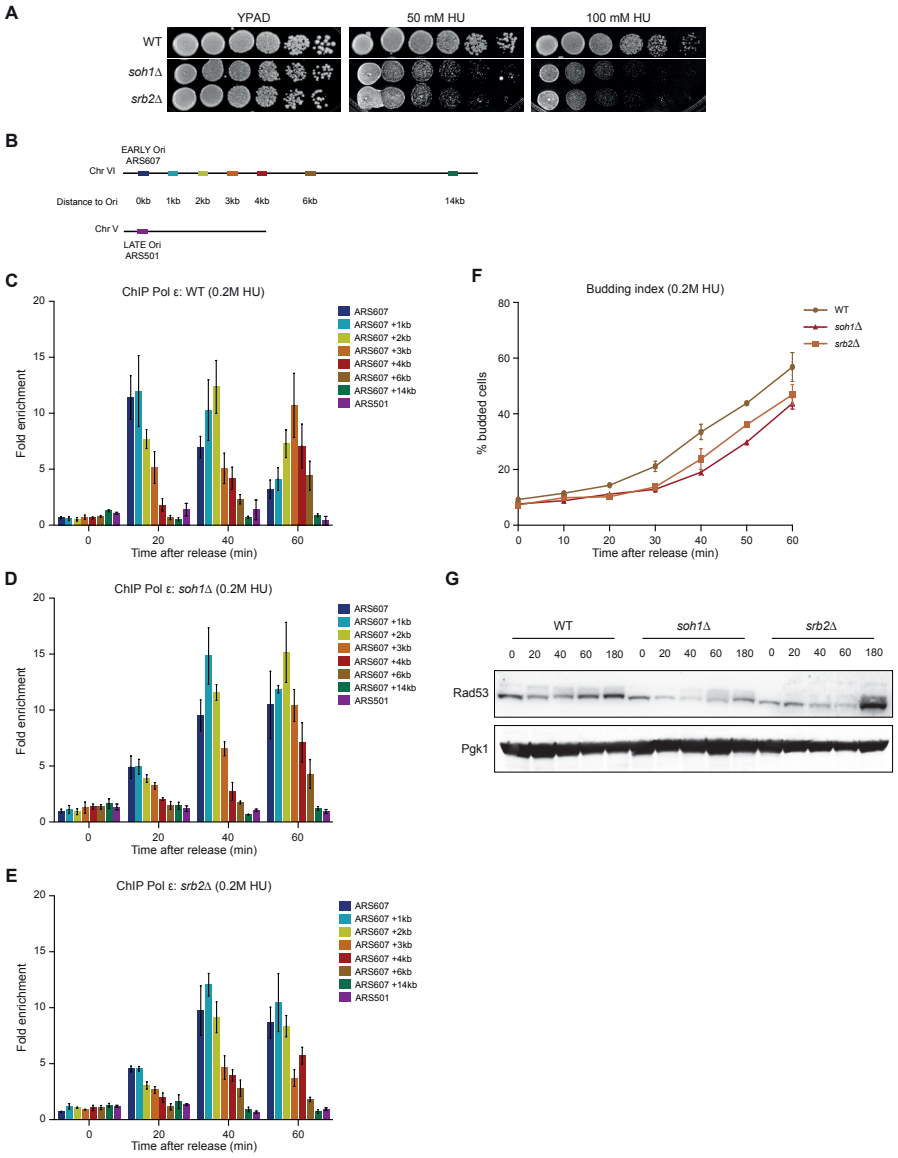

Figure 3. Replication stress effects in *de novo* Mediator mutants.
(A) Spot dilution assay for *de novo* mutants of *soh1Δ* and *srb2Δ*. Cells were diluted and spotted on untreated plates and on plates containing 50 mM and 100 mM HU. (B) Overview of ChIP-qPCR at ARS607 and ARS501. (C-E) ChIP-qPCR analysis of Pol ε at ARS607 and ARS501 for (C) WT, (D) *soh1Δ* (E) *srb2Δ* strains. Data represent the mean relative fold enrichment of Myc signal over IgG signal in at least three independent experiments ± s.e.m. Values were normalized to unreplicated regions (ARS607+14kb). (F) Budding index for WT, *soh1Δ* and *srb2Δ* strains arrested in G1-phase and released in S-phase in 0.2M HU. Data are represented from three independent experiments ± s.e.m. (G) Western blot analysis of Rad53 activation in WT, *soh1Δ* and *srb2Δ* strains.

Mediator mutants can recover from HU-induced fork stalling

Mec1-Ddc2 are recruited to HU-stalled replication forks to activate the intra-S-phase checkpoint and protect forks from collapse, thereby ensuring a proper restart (Can et al., 2019; De Piccoli et al., 2012; Zhou et al., 2016; Zou and Elledge, 2003). The increased Ddc2 levels in Mediator mutants after recovery from HU suggest are indicative of an increase in stalled/collapsed forks. To investigate if Mediator mutants can recover from HU-induced replication fork stalling, we assessed colony formation following a 2-hour HU exposure. Remarkably, the *soh1Δ* and *srb2Δ* mutants were able to fully recover from the HU-induced replication stress (Supplementary Figure 2B). Thus, loss of Mediator delays both DNA replication and activation of the intra-S-phase checkpoint following HU exposure but does not affect the recovery of cells from HU-induced replication fork slow down.

Mediator does not associate with replication forks but is removed from promoters in response to HU

Given that replication fork progression is delayed and Ddc2 foci are increased after loss of Mediator, we next sought to address whether Mediator acts directly at replication forks. To this end, we performed ChIP-qPCR of Myc-tagged Soh1, which served as a proxy for Mediator's localization on chromatin. Unlike Pol ε, Soh1 was neither enriched directly at origins of replication, nor at any of their distal regions in G1 or S-phase cells (Figure 4A).

Since Mediator could not be detected at stalled replication forks, we hypothesized that its potential role in preventing replication stress may be link to its function in transcription. To assess this, we examined Mediator's presence at the highly transcribed genes *EFB1, GLY1* and *HSP150,* which are known to be bound by Mediator, in G1 and HU-treated S-phase cells (Grünberg et al., 2016). High levels of Soh1 recruitment at both *EFB1* and *GLY1* promoter regions were observed in G1, whereas somewhat lower levels of Soh1 were observed at the *HSP15*0 promotor region. However, after release in S-phase in the presence of HU, Soh1-Myc levels at *EFB1, GLY1* and *HSP150* promoter regions were decreased (Figure 4B), suggesting that following HU-induced replication stress Mediator is removed from chromatin. A similar observation was made for RNAPII, which is also removed from chromatin during replication stress (Poli et al., 2016). This suggests that Mediator, likely together with RNAPII, is unloaded from chromatin in response to HU-induced replication stress.

Transcriptome changes in Mediator mutants neither affect DNA replication nor the DNA damage response

Mediator's removal from promoters during replication stress could be required for the transcriptional response upon replication stress. Mediator controls transcription through its Head and Middle modules that interact with RNAPII and several general transcription factors, while its tail contacts

sequence-specific transcription factors. It thereby bridges transcriptional activators bound to enhancer regions and the general transcription machinery at core promoters (Jeronimo et al., 2016; Petrenko et al., 2016). This promotes the assembly of the preinitiation complex (PIC) and controls transcription initiation (reviewed in (Soutourina, 2018). Based on this, we investigated whether transcriptional changes in the absence of Mediator could explain the increased HU sensitivity and increased replication stress levels as measured by Ddc2 foci analysis. We performed RNA-seq in *soh1Δ* and *srb2Δ* mutants in untreated G1-phase and HU-treated S-phase cells. In G1-phase, we observed a lower expression of 311 and 443 genes in *soh1Δ* and *srb2Δ*, respectively, when compared with WT (Padjust <0.01 and fold change >2). In S-phase, we observed a lower expression of 308 and 346 genes *soh1Δ* and *srb2Δ*, respectively, when compared with WT (Padjust <0.01 and fold change >2). These changes largely overlapped between the two mutants (Figure 4C).

We also observed that the transition from G1- to S-phase induces a large transcriptional change, with 709 genes changing expression by 2-fold in WT. When analyzing these changes under replication stress conditions in WT and Mediator mutants, we observed very high correlations (r^2=0.9) between the transcriptional changes from G1- to S-phase in WT cells versus *soh1Δ* or *srb2Δ* (Figure 4D-E). Thus, while loss of Mediator regulates transcription of a large number of genes, the changes in gene expression underlying the transition from G1- to S-phase remained unaffected following loss of Mediator.

Because Mediator plays a role in transcription elongation as well as transcription initiation (Conaway and Conaway, 2013), we investigated if loss of Mediator especially affects the expression of longer genes. We compared the gene length of the downregulated genes in the Mediator mutants to that in WT cells. The median length of the 325 affected genes was similar to the median gene length of 1kb, indicating that Mediator does not affect the expression of longer genes in particular (Figure 4F).

Next, we identified the biological networks affected by the transcriptional changes observed after loss of Mediator. We performed SAFE analysis on the transcriptome changes in all tested conditions and visualized the GO biological process map. During G1-phase, loss of Mediator did not lead to the enrichment of a single biological network region (Supplementary Figure 3A-B). On the contrary, following HU treatment there is enrichment in the transcription and chromatin organization network (Supplementary Figure 3C-D). However, genes in this cluster that that show lower expression, such as for instance *WTM1*, *GAL4*, *RMG1* and *EMI2*, do not have any link to DNA replication or repair. Upon further inspection, *CDC6* is the only gene involved in DNA replication that is around 2-fold lower in its expression. Since the Cdc6 protein becomes degraded during S-phase (Drury et al., 1997), its decreased expression during HU treatment likely will not contribute to the observed increase in replication stress in Mediator mutants.

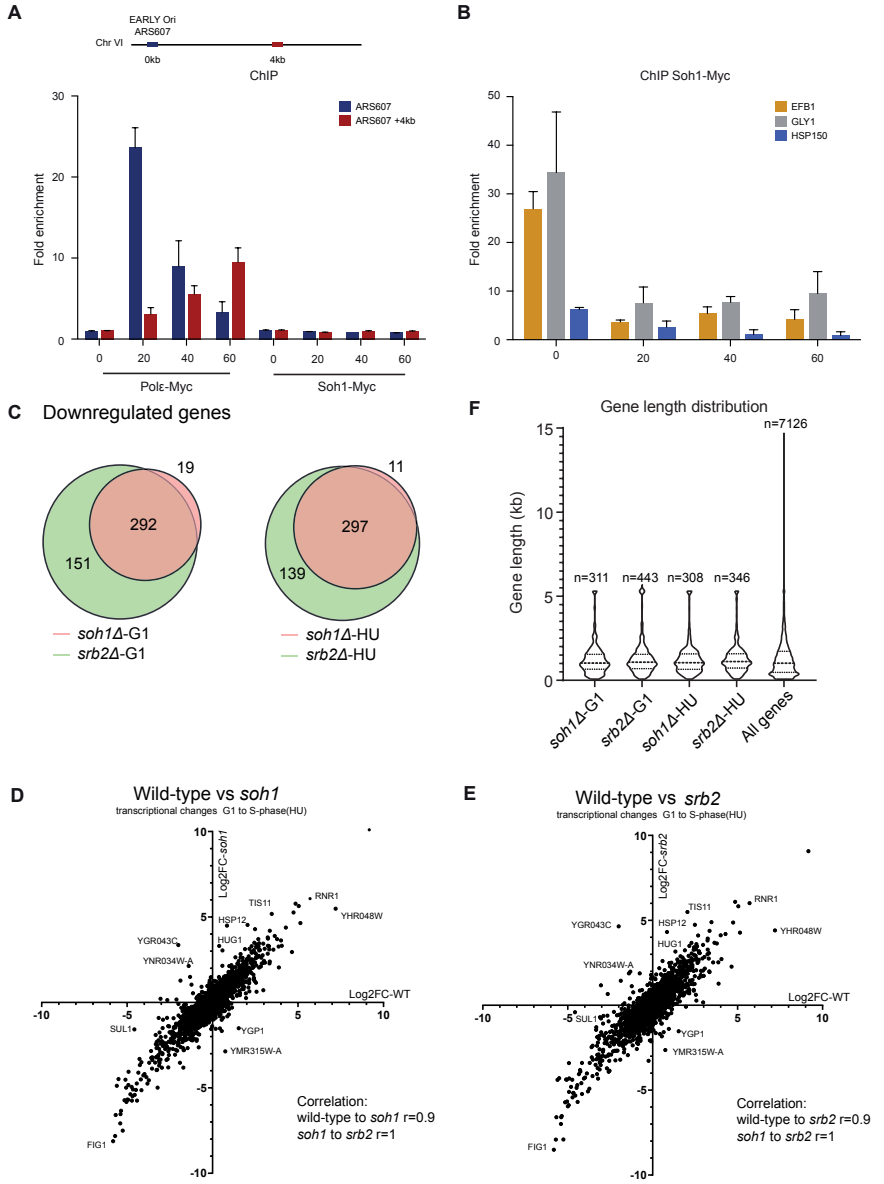

Figure 4. Localization of Soh1 and Rbp1, and RNA-seq analysis of *soh1Δ* and *soh1Δ* mutants.
(A) ChIP-qPCR analysis of Pol ε and Soh1 at ARS607. Data represent the mean relative fold enrichment of Myc signal over IgG signal in at least three independent experiments ± s.e.m. Values were normalized to unreplicated regions (ARS607+14kb). (B) ChIP-qPCR analysis of Soh1 at gene promoters normalized to SMC2. Data are represented as the mean fold enrichment from three independent experiments ± s.e.m. (C) Venn diagrams of downregulated genes identified by RNA-seq in *soh1Δ* and *srb2Δ* strains in G1-phase and HU-treated S-phase cells. Correlation plot of transcriptome changes from G1-phase and HU-treated S-phase between WT and (D) *soh1Δ* and (E) *srb2Δ* strains. (F) Violin plots of gene length distribution of the downregulated genes in *soh1Δ* and *srb2Δ* strains and gene length of all genes.

Mediator mutants show a reduced RNAPII release from chromatin following replication stress

Mediator recruits RNAPII to promoters (Biddick et al., 2008; Esnault et al., 2008) and loss of Mediator affects RNAPII levels at active genes (Eyboulet et al., 2013). Since impaired removal of RNAPII on chromatin leads to conflicts between replication and transcription, we investigated RNAPII levels in Mediator mutants (Felipe-Abrio et al., 2015; Landsverk et al., 2020; Poli et al., 2016). We performed RNAPII chromatin immunoprecipitation sequencing (ChIP-seq) of Rbp1 (the largest subunit of RNAPII) during untreated G1 and HU-treated S-phase WT and *soh1Δ* mutant cells. The distribution of RNAPII across the gene body as determined by ChIP-seq was plotted from transcription start sites (TSS) to transcription termination sites (TES) (Figure 5A and Supplementary Figure 4). Consistent with previous observations and the downregulation of genes in the RNA-seq, we see a reduced occupancy of RNAPII in *soh1Δ* mutants (Figure 5A-B), especially across differentially expressed genes in G1, albeit that loss of RNAPII was not observed at TES in non-affected genes (Figure 5C-D) (Knoll et al., 2018). We conclude that the transcriptional changes in Mediator mutants are likely a direct effect of decreased RNAPII occupancy at these genes. When compared to G1-phase cells, HU-treated S-phase cells showed a more modest loss of RNAPII across differentially expressed genes in the absence of Soh1 (Figure 5B-D). Moreover, at the non-affected genes RNAPII levels even increased at the TSS, but not the TES, in *soh1Δ* when compared to that in WT (Figure 5B-D). We infer that Mediator has a strong impact on maintaining proper RNAPII levels on chromatin in G1-phase cells, whereas in HU-treated S-phase cells, RNAPII levels are increased near the TSS in the absence of Soh1. Consequently, Mediator loss leads to a more profound retention of RNAPII in S-phase cells, thereby interfering with the progression of DNA replication.

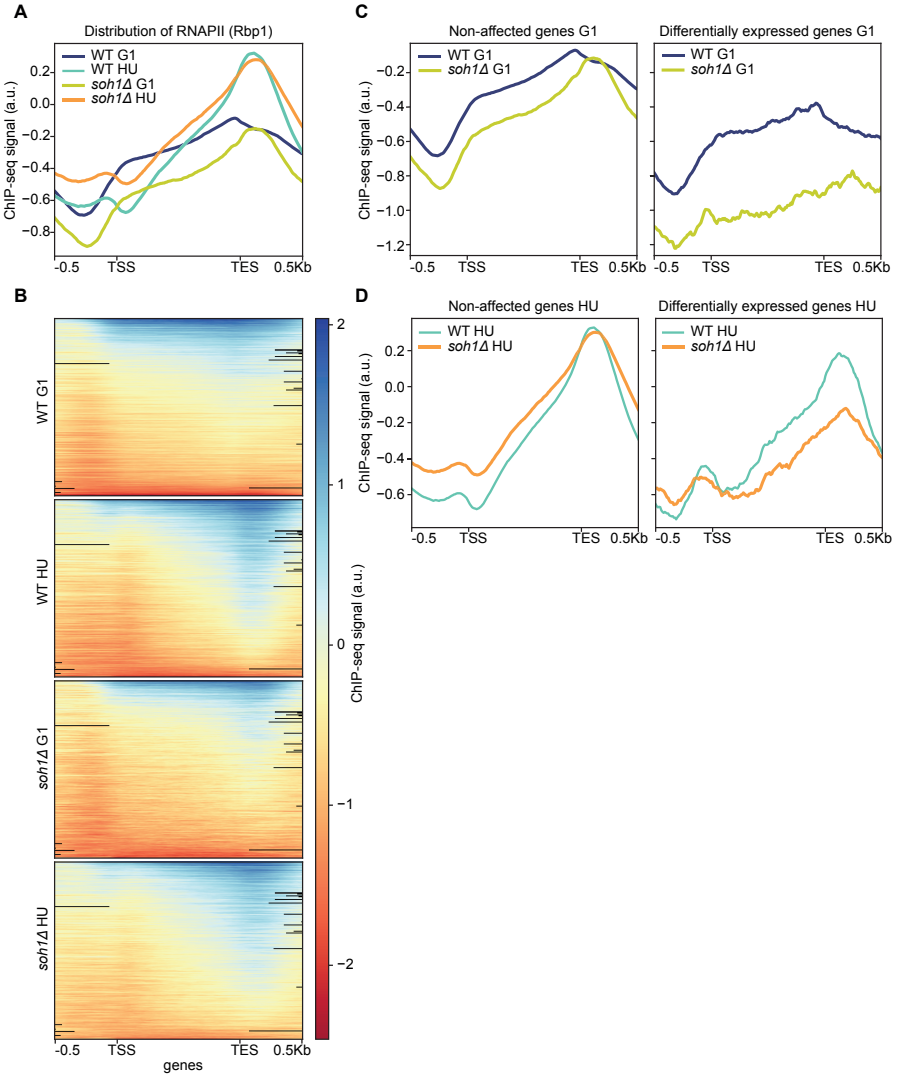

Figure 5. Decreased RNAPII occupancy in *soh1Δ* mutants.
(A) ChIP-seq results of Rbp1 enrichment plotted over the gene body in WT and *soh1Δ* in G1-phase and HU-treated S-phase cells. (B) Heatmaps plotted over gene body from Rbp1 ChIP-seq data plotted over the gene body in WT and *soh1Δ* in G1-phase and HU-treated S-phase cells. (C) Rbp1 occupancy binding across genes unaffected in expression (left) and affected genes (right) in *soh1Δ* mutants during G1-phase. (C) Rbp1 occupancy binding across genes unaffected in expression (left) and affected genes (right) in *soh1Δ* mutants during HU-treated S-phase cells.

Mediator mutants accumulate R-loops and gives rise to replication stress

When the nascent mRNA hybridizes with the template DNA, co-transcriptional RNA-DNA hybrids (R-loops) are formed (Santos-Pereira and Aguilera, 2015). R-loops can block replication fork progression and are a source of genome instability. Recently, it has been suggested that R-loops formed near the TES interfere with replication fork progression, leading to increased γH2AX and phospho-RPA32 (S4/S8) levels (Promonet et al., 2020). Because of Mediator's role in the regulation of RNAPII chromatin occupancy, especially near the TES, we questioned whether this coincides with an increase in R-loops in the absence of Mediator.

To investigate the accumulation of R-loops at individual genes we employed DNA-RNA immunoprecipitation (DRIP) with the S9.6 antibody in Mediator mutants. DRIP-qPCR was performed in G1-phase and HU treated S-phase cells and R-loops were quantified at the highly transcribed *SPF1*, *GCN4*, *PDC1* and *PDR5* genes. These genes have previously been shown to accumulate R-loops and their expression was not affected by loss of Mediator (García-Benítez et al., 2017) (Figure 6A, Supplementary Figure 4 and Supplementary File 1). In WT cells, low R-loop signals were observed at the tested genes and *in vitro* RNase H treatment decreased the R-loop levels at these genes, indicating specificity of the signal. In contrast, in *soh1Δ* or *srb2Δ* cells, R-loops levels were highly increased at all genes in both G1- and HU-treated S-phase cells, and this increase was not limited to TES regions (Figure 6B). This indicates that Mediator prevents the accumulation of R-loops near TSS, gene bodies and TES. To determine if the alleviation of R-loops in Mediator subunits decreases replication stress levels, we scored the formation of Ddc2 foci after HU treatment in the presence and absence of RNase H1 overexpression, which specifically removes R-loops. Similar to our earlier observations (Figure 2D), Ddc2 foci were increased in *soh1Δ* and *srb2Δ* mutants (Figure 6C). However, RNase H1 overexpression prior to HU exposure significantly reduced Ddc2 foci levels in *soh1Δ* and *srb2Δ* cells levels, demonstrating that Mediator prevents R-loop formation and thereby replication stress. Detrimental R-loops are especially formed near the TES, causing replication fork stalling after collisions between RNA and DNA polymerases (Promonet et al., 2020). Consequently, our results may suggest that Mediator ensures proper RNAPII unloading, thereby preventing retention of RNAPII and the formation of R-loops, which can cause replication fork stalling particularly following treatment of cells with HU.

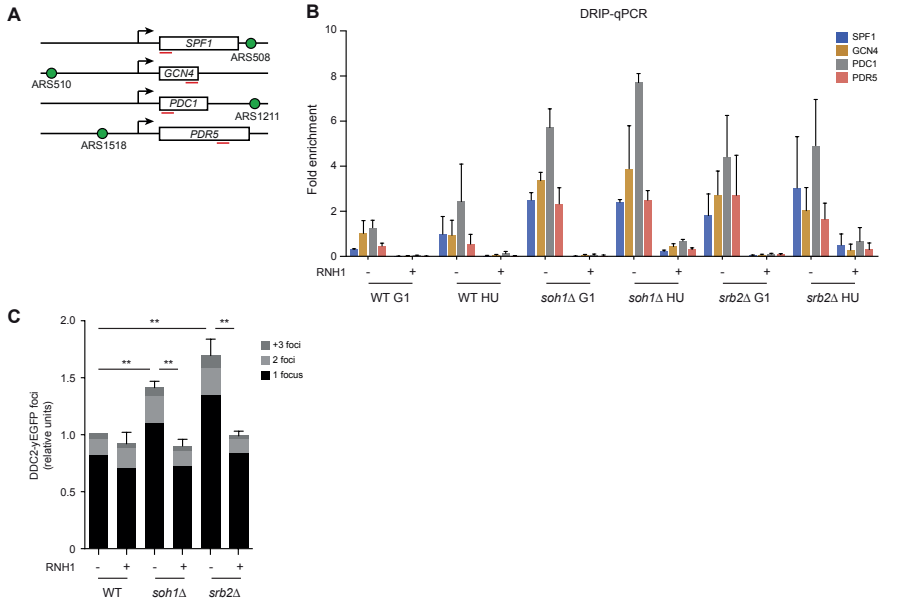

Figure 6. DRIP-seq and Ddc2 foci formation in *soh1Δ* and *srb2Δ* mutants.
(A) DRIP-qPCR analysis of R-loops at various genes in *soh1Δ* and *srb2Δ* strains in G1 and S-phase. Data are represented as the mean percent input method (El Hage and Tollervey, 2018) from two independent experiments ± s.e.m. (B) Ddc2 foci formation was scored after treating *soh1Δ* and *srb2Δ* mutants with HU and letting them recover for 2 hours. RNAse H1 expression was induced prior to HU treatment by letting cells grow in galactose.

DISCUSSION

In this study, we surveyed which yeast deletion and DaMP mutants show increased HU sensitivity. We found 285 out of ~7000 mutants to be HU sensitive, including several mutants of known regulators of responses to DNA replication stress Rad54, Rad51, Pol32 and Ino80, (Lydeard et al., 2007; Poli et al., 2017). We performed a focused follow-up screen to identify mutants that display HU sensitivity because they fail to resolve stalled replication forks, a process that was monitored by scoring Ddc2 foci after HU treatment. This Ddc2 screen showed 45 out of 85 mutants with at least a 20% increase in Ddc2 foci formation. Among these were several mutants in genes encoding different subunits of the clathrin and Mediator complexes. The clathrin complex members were previously found to be sensitive to HU, but gene interaction analysis suggested they reduce HU-induced stress by functioning in vacuolar trafficking (Hartman and Tippery, 2004). However, since clathrin complex mutants show elevated levels of Ddc2 foci, this suggests they not only indirectly affect the response to HU-induced stress,

but also directly contribute to replication fork stability under conditions of HU. Further research is required to elucidate how these mutants, and consequently endocytosis, contribute to replication fork maintenance following replication stress. Since Mediator had not been linked to replication stress, we further investigated the role of Mediator in preventing DNA replication stress. We observed increased RNAPII retention and increased R-loop formation following HU in the absence of Mediator complex members. Alleviation of R-loops by RNH1 overexpression relieved replication stress in Mediator mutants, suggesting that Mediator functions to prevent R-loop formation, thereby preserving replication fork progression.

The Mediator complex consists of 25 (yeast) or 30 (human) subunits that are grouped into four modules: Head, Middle, Tail and CDK8 Kinase (reviewed in (Jeronimo and Robert, 2017). Together with RNAPII and other transcription factors, Mediator coordinates transcription initiation (Jeronimo and Robert, 2017). While Mediator mutants were previously found to be sensitive to HU, the role of Mediator in the replication stress response remained elusive (Chang et al., 2002; Hartman and Tippery, 2004; Parsons et al., 2004; Woolstencroft et al., 2006). Since Mediator plays an important role in transcription regulation, we investigated transcriptome changes in *soh1Δ* and *srb2Δ* mutants. In both untreated G1-phase and HU-treated S-phase cells, transcriptome changes were not enriched for genes involved in DNA replication or DNA damage repair, which is in line with previous observations (Koschubs et al., 2009; Santos-Rosa et al., 1996). Moreover, the transcriptional changes accompanying the transition from G1 to S-phase in these mutants were highly similar to wild-type (r^2=0.9). This suggests that the sensitivity of Mediator mutants to HU-induced replication stress is not due their effect on the transcriptome. While Mediator is not present at replication forks, it binds chromatin where it frequently associates with RNAPII. However, our results suggest that Mediator, similar to RNAPII, is removed from chromatin following an HU treatment of cells (Poli et al., 2016). We therefore checked RNAPII levels (by monitoring Rpb1 using ChIP-seq) on chromatin in the absence of Mediator. Strikingly, RNAPII levels were lower in Mediator mutants, in agreement with other reports (Eyboulet et al., 2013; Guglielmi et al., 2007; Petrenko et al., 2017). In the case of *soh1Δ*, this is likely due to loss of the interaction between Soh1 and the CTD domain of Rpb1 in the RNAPII complex (Tsai et al., 2017). Even though global RNAPII levels are decreased, during replication stress Mediator mutants retained higher levels of RNAPII, particularly near the TES. Impaired removal of RNAPII during replicative stress affects replication fork progression and is associated with a decrease in replication fork speed and delayed checkpoint activation, which are all phenotypes that have also been observed in Mediator mutants (Felipe-Abrio et al., 2015; Poli et al., 2016). In addition to RNAPII blocking replication fork progression, R-loops are also obstacles for the replication machinery (Prado and Aguilera, 2005). Especially, R-loops formed near the TES can cause genome instability (Promonet

et al., 2020). Since Mediator affects RNAPII levels near the TES in untreated conditions, we investigated R-loop formation and found elevated R-loop levels in Mediator mutants. Removal of R-loops by Rnase H overexpression alleviated the formation of Ddc2 foci in Mediator mutants, suggesting R-loops are the cause of replication stress in these mutants. Further research is required to investigate whether the increased RNAPII on chromatin could be linked to detrimental R-loop formation in Mediator mutants. For example, ChIP-seq may confirm whether R-loops are formed at RNAPII retention sites and if these coincide with stalled or collapsed forks as measured by RPA (stalled forks) or Rad52 (collapsed forks). Since Mediator mutants do not show a defect in recovery from HU exposure, the replication stress measured in these mutants might reflect stalled forks, capable of eventually resuming DNA replication after a release from HU.

R-loops may also accumulate in Mediator mutants due to a defect in a process called gene gating. During gene gating, transcribed genes are targeted to the nucleopore complex (NPC) to promote the direct export of the messenger ribonucleoprotein particle (mRNP). This suppresses R-loop formation because it prevents the back-hybridization of the nascent RNA with the DNA (Gaillard et al., 2017; García-Benítez et al., 2017). In the absence of the mRNA export complex TREX-2, gene gating is impaired and this leads to transcription- and R-loop- and hyperrecombination (Gallardo et al., 2003; González-Aguilera et al., 2008). The TREX-2 subunit Sac3 physically interacts with the Mediator subunit Soh1 and when this interaction is lost, gene gating is impaired (Schneider et al., 2015). Therefore, Mediator may prevent the accumulation of R-loops by promoting gene gating. In the absence of gene gating, artificial tethering of DNA to the NPC suppresses R-loop formation (García-Benítez et al., 2017). Since Mediator mutants contain high levels of R-loops, targeting R-loop containing genes to the NCP could alleviate R-loop formation and replication stress in these mutants. Interestingly, mutants in which gene gating is impaired show decreased levels of RNAPII at genes containing R-loops (García-Benítez et al., 2017). Thus, a potential defect in gene gating could also explain the decreased global loading of RNAPII in Mediator mutants. Taken together, we propose a mechanism in which Mediator promotes gene gating, thereby suppressing R-loop formation and preventing replication stress (Figure 7). To understand if Mediator prevents R-loop formation through efficient gene gating and/or by promoting RNAPII removal from genes, further research will be required. To this end, it is interesting to note that Mediator, through its general role in transcription, is implicated in preventing various diseases, including developmental disorders and cancer (Brägelmann et al., 2017; Hashimoto et al., 2011; Risheg et al., 2007; Syring et al., 2016). Future studies may therefore also unravel whether Mediator's role in counteracting replication stress is conserved to humans and contributes to preventing disease development.

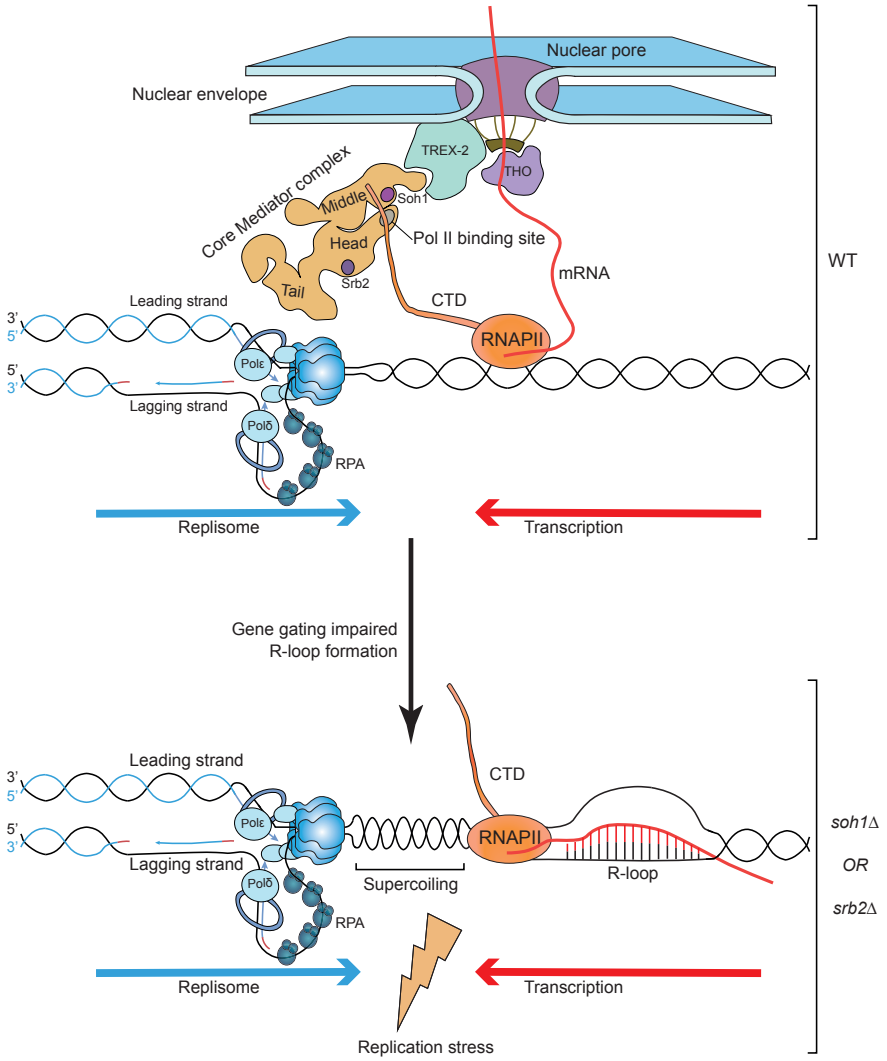

Figure 7. Model proposing how the Mediator complex prevents R-loop formation.
Model illustrating the role of Mediator in gene gating. In WT cells (top panel), Mediator subunit Soh1 binds the TREX-2 complex to position RNAPII and the nascent mRNA at the nuclear pore, thereby preventing R-loop formation. The incoming replisome (left) is able to pass RNAPII without transcription-replication collisions. In the absence of subunits Soh1 or Srb2 (bottom panel), the Mediator complex cannot bind TREX-2 and RNAPII properly. Gene gating is impaired and the nascent mRNA can hybridize with the template DNA. The R-loop induces supercoiling between the replisome and RNAPII and prevent passage of the replisome. This leads to a head-on collision between the replisome and RNAPII, leading the replication stress.

EXPERIMENTAL PROCEDURES

Yeast strains, plasmid and antibodies

Yeast strains and primers used in this study are listed in Table 1 and 2. Yeast strains that were used initial validation studies were taken from the yeast knockout (YKO) library (Tong and Boone, 2006). pRS416-GAL1-RNH1 (gift from Andrés Aguilera) was digested with *SalI-HF* and *KpnI-HF* (New England Biolab) to obtain GAL1p-RNH1-CYCt. The digested product was ligated into pRS314 *SalI* and *KpnI* sites to obtain pRS314-GAL1-RNH1. Antibodies used were anti-myc 9B11 (#2276, Cell Signaling, Leiden, the Netherlands), anti-Rad53 (#ab104232; Abcam, Cambridge, UK), anti-Pgk1 (#459250; Invitrogen, Carlsbad, CA), anti-Rbp1 (ab817, Abcam, Cambridge, UK) and monoclonal mouse antibody S9.6 (MABE1095, Merck Millipore, Darmstadt, Germany).

Yeast deletion library screen

Yeast deletion and DaMP libraries were pinned in 1536 format on YPAD plates with or without 150 mM HU using a RoToR from Singer Instruments (Watchet, UK). After three days, plates were photographed. Colony sizes quantification, plate normalization and correction for spatial and border effects was performed with the MATLAB Colony Analyzer (Bean et al., 2014). Statistical significance was performed with a Welch T-Test and corrected for multiple testing using the Benjamini Hochberg method. The difference in colony size in treated versus untreated yeast mutants was calculated in size percentage difference from untreated. All analysis was performed in MATLAB software.

Venn diagrams

Venn diagrams were created using InteractiVenn (Heberle et al., 2015).

SAFE analysis

SAFE analysis was performed as previously described (Baryshnikova, 2018) by integrating the chemical genomic data from the HU screen or the transcriptional changes from RNA-seq to the genetic interaction similarity network (Costanzo et al., 2016) annotated with the Gene Ontology biological process terms.

Spot dilution test

Cells were grown to mid-log in rich media (YPAD) collected and set to concentration of 2.5 x 10^8/ml, 10-fold serial dilutions were generated and spotted on plate containing rich YPAD and YPAD containing HU and were grown for 3 days respectively at 30 ˚C.

Ddc2 focus formation screen

A subset of mutants from the yeast knock out collection (Supplemental Table 1) was crossed with a Ddc2-yEGFP strain containing synthetic genetic array (SGA) anti-diploid selection markers and a URA3 selection marker using synthetic genetic array (SGA) procedures (Tong and Boone, 2006). Library handling and crosses were performed using a RoToR from Singer Instruments (Watchet, UK). Strains containing endogenously tagged Ddc2-GFP were grown to mid-log, synchronized with YPAD containing α-factor for 2 hours, washed and released in YPAD containing 0.2 M HU (Sigma-Aldrich) for 1h, cells were allowed to recover in YPAD for 2h. Cells were collected and fixed in 4% paraformaldehyde at room temperature for 15 minutes, washed and resuspended in KPO4/Sorbitol solution (10 mM KPO4, 1.2 M Sorbitol, pH=7.5). Images were captured with a Zeiss AxioImager M2 widefield fluorescence microscope equipped with 100x PLAN APO (1.4 NA) oil-immersion objectives (Zeiss) and an HXP 120 metal-halide lamp used for excitation. 21 focal steps of 0.25μm were acquired with an exposure time of 1000 ms using a GFP/YFP 488 filter (excitation filter: 470/40 nm, dichroic mirror: 495 nm, emission filter: 525/50 nm). Images were recorded using ZEN 2012 software and analyzed with Fiji.

Replication ChIP-qPCR

ChIP was performed as previously described (Cobb and van Attikum, 2010). Briefly, cells were grown for 3 hours, treated with α-factor for 2 hours, washed once in YPAD medium and released in YPAD containing 0.2M HU. Samples were collected at 0, 20, 40 and 60 minutes after release. For 20ºC replication ChIP-qPCR, cells were grown for 3 hours at 30 ºC, treated with α-factor for 2 hours at 20 ºC, washed once in YPAD medium and released in YPAD at 20ºC. Samples were collected at 0, 25, 30, 35 and 40 minutes. Cells were fixed with 1% formaldehyde. Input and immunoprecipitated DNA was purified and analyzed by quantitative (q)PCR using primers listed in Table 2. Relative enrichment was determined by 2^{-DDCt} method. Signal for Dynabeads alone was used to correct for background.

Copy number assay

Cells were grown for 3 hours, treated with α-factor for 2 hours, washed once in YPAD medium and released in YPAD containing 0.2M HU. 2,5 x 10^7 cells were collected at 0, 20, 40 and 60 minutes after release from G1, fixed with sodium azide and washed with 10mM Tris, 50mM EDTA. For genomic DNA extraction, cells were digested in 1M Sorbitol, 0.1M Sodium citrate pH 7.0, 60mM EDTA, 8mg/ml β-Mercaptoethanol, 2mg/ml Zymolyase 20T for 45 min, and DNA was isolated using the Qiagen DNeasy Blood and Tissue kit following the manufacturer

instructions. The amount of genomic DNA at ARS607 and downstream loci was quantified by qPCR using the ratio of DNA in HU-arrested to that in G1 and normalized to ARS607+14kb locus.

Budding index

Cells were grown for 3 hours and treated with α-factor for 2 hours, washed once in YPAD medium and released in YPAD only or YPAD containing 0.2M HU. Samples were taken every 10 minutes for 2 hours and fixed in 4% paraformaldehyde at room temperature for 15 minutes, washed and resuspended in KPO4/Sorbitol solution (10 mM KPO4, 1.2 M Sorbitol, pH=7.5). Brightfield images were captured with a Zeiss AxioImager M2 widefield fluorescence microscope equipped with 100x PLAN APO (1.4 NA) oil-immersion objectives (Zeiss).

ChIP sequencing (ChIP-seq)

ChIP was performed as previously described. Input and IP samples were prepared using the Kapa Hyper Prep kit and sequenced on Illumina NovaSeq6000 PE 2x150. Reads were trimmed using and aligned to the UCSC SacCer3 reference genome (April 2011) with BWA (version: 0.7.16a-r1181) using default options. MACS2 (version 2.1.1.20160309) was used to call peaks (Zhang et al., 2008). TSS – TES enrichment plots were made using scaled normalization (SES) with DeepTools on the Galaxy server (Ramírez et al., 2016).

RNA sequencing (RNA-seq)

Three independent yeast colonies were used for inoculation. Overnight cultures were diluted in fresh medium. Cells were grown for 3 hours, treated with α-factor for 2 hours, washed once in YPAD medium and released in YPAD containing 0.2M HU. Samples were collected after α-factor synchronization and after release of 60 minutes in HU. Total RNA was isolated using the RNeasyMini kit (Qiagen) and treated with the RNase-Free DNase Set (Qiagen) to remove any contaminating genomic DNA. Library preparations were performed with the NEBNext Ultra II Directional RNA Library Prep Kit (Illumina). Three independent biological replicates for each condition were subjected to RNA-seq analysis using an Illumina NovaSeq600. Reads were aligned to the UCSC SacCer3 reference genome (April 2011) using Tophat20 with the following parameters "-G SacCer3_SGD.gtf -I 1000 -i 20 -p 6 -o", and counted with HTSeq with the following parameters "htseq-count -f bam --stranded=yes". Differential expression was analysed in R by DESeq2 (Love et al., 2014) using the default parameters, including Benjamini-Hochberg procedure for correcting p-values for multiple testing.

Western blot analysis

Cells were grown for 3 hours, synchronized with α-factor for 2 hours, washed with YPAD and released in YPAD containing 0.2 M HU. Samples were collected at 0, 20, 40, 60 and 120 minutes after release. Whole cell extracts were prepared by TCA precipitation and analyzed by SDS-PAGE.

DRIP-qPCR

DRIP-qPCR was performed as previously described (El Hage and Tollervey, 2018). Briefly, cells were grown for 3 hours, treated with α-factor for 2 hours, washed once in YPAD medium and released in YPAD containing 0.2M HU. Samples were collected at 0 and 60 minutes after release and fixed with sodium azide. Cells were spheroplasted, lysed and treated with Proteinase K. DNA isolated by spooling precipitated DNA on on a glass rod, washing twice with 70% EtOH and gently resuspending in TE. DNA was fragmented overnight by a cocktail of restriction enzymes and half was treated with RNAse H1. IP was performed using monoclonal mouse antibody S9.6 coupled to protein A magnetic beads (Invitrogen). Input and immunoprecipitated DNA was purified and analyzed by quantitative (q)PCR using primers listed in Table 2.

ACKNOWLEDGEMENTS

This work was financially supported by an ERC Consolidator grant and NWO VICI grant to H.v.A..

CONFLICT OF INTEREST

The authors declare that they have no conflicts of interest with the contents of this article.

AUTHOR CONTRIBUTIONS

A.B. performed Ddc2 foci experiments, SAFE analysis, strain construction, spot dilution assays, western blots, RNA-seq analysis, ChIP experiments, ChIP-seq analysis, DRIP-qPCR experiments and wrote the paper. L.K. performed the HU screen and analysis, spot dilution assays, RNA-seq analysis, ChIP experiments, ChIP-seq analysis, DRIP-qPCR experiments, and wrote the paper. M.T.E performed copy number assays and ChIP experiments. S.M.S helped with the HU screen analysis. D.v.H performed strain construction, ChIP and Ddc2 foci experiments. M.M performed strain and plasmid construction, budding index and Ddc2 foci experiments and western blots. H.v.A. supervised the project and wrote the paper.

REFERENCES

1. Baryshnikova, A. (2018). Spatial Analysis of Functional Enrichment (SAFE) in Large Biological Networks. Methods in molecular biology (Clifton, NJ) *1819*, 249-268.

2. Bean, G.J., Jaeger, P.A., Bahr, S., and Ideker, T. (2014). Development of ultra-high-density screening tools for microbial "omics". PLoS One *9*, e85177.

3. Biddick, R.K., Law, G.L., Chin, K.K.B., and Young, E.T. (2008). The transcriptional coactivators SAGA, SWI/SNF, and mediator make distinct contributions to activation of glucose-repressed genes. The Journal of biological chemistry *283*, 33101-33109.

4. Bjergbaek, L., Cobb, J.A., Tsai-Pflugfelder, M., and Gasser, S.M. (2005). Mechanistically distinct roles for Sgs1p in checkpoint activation and replication fork maintenance. The EMBO journal *24*, 405-417.

5. Brägelmann, J., Klümper, N., Offermann, A., von Mässenhausen, A., Böhm, D., Deng, M., Queisser, A., Sanders, C., Syring, I., Merseburger, A.S.*, et al.* (2017). Pan-Cancer Analysis of the Mediator Complex Transcriptome Identifies CDK19 and CDK8 as Therapeutic Targets in Advanced Prostate Cancer. Clin Cancer Res *23*, 1829-1840.

6. Can, G., Kauerhof, A.C., Macak, D., and Zegerman, P. (2019). Helicase Subunit Cdc45 Targets the Checkpoint Kinase Rad53 to Both Replication Initiation and Elongation Complexes after Fork Stalling. Mol Cell *73*, 562-573.e563.

7. Carter, C.D., Kitchen, L.E., Au, W.C., Babic, C.M., and Basrai, M.A. (2005). Loss of SOD1 and LYS7 sensitizes Saccharomyces cerevisiae to hydroxyurea and DNA damage agents and downregulates MEC1 pathway effectors. Mol Cell Biol *25*, 10273-10285.

8. Cevher, M.A., Shi, Y., Li, D., Chait, B.T., Malik, S., and Roeder, R.G. (2014). Reconstitution of active human core Mediator complex reveals a critical role of the MED14 subunit. Nat Struct Mol Biol *21*, 1028-1034.

9. Chang, M., Bellaoui, M., Boone, C., and Brown, G.W. (2002). A genome-wide screen for methyl methanesulfonate-sensitive mutants reveals genes required for S phase progression in the presence of DNA damage. Proceedings of the National Academy of Sciences of the United States of America *99*, 16934-16939.

10. Cobb, J., and van Attikum, H. (2010). Mapping genomic targets of DNA helicases by chromatin immunoprecipitation in Saccharomyces cerevisiae. Methods in molecular biology (Clifton, NJ) *587*, 113-126.

11. Conaway, R.C., and Conaway, J.W. (2013). The Mediator complex and transcription elongation. Biochimica et biophysica acta *1829*, 69-75.

12. Costanzo, M., VanderSluis, B., Koch, E.N., Baryshnikova, A., Pons, C., Tan, G., Wang, W., Usaj, M., Hanchard, J., Lee, S.D.*, et al.* (2016). A global genetic interaction network maps a wiring diagram of cellular function. Science (New York, NY) *353*, aaf1420.

13. De Piccoli, G., Katou, Y., Itoh, T., Nakato, R., Shirahige, K., and Labib, K. (2012). Replisome stability at defective DNA replication forks is independent of S phase checkpoint kinases. Molecular cell *45*, 696-704.

14. Drury, L.S., Perkins, G., and Diffley, J.F. (1997). The Cdc4/34/53 pathway targets Cdc6p for proteolysis in budding yeast. Embo j *16*, 5966-5976.

15. El Hage, A., and Tollervey, D. (2018). Immunoprecipitation of RNA:DNA Hybrids from Budding Yeast. Methods in molecular biology (Clifton, NJ) *1703*, 109-129.

16. Esnault, C., Ghavi-Helm, Y., Brun, S., Soutourina, J., Van Berkum, N., Boschiero, C., Holstege, F., and Werner, M. (2008). Mediator-dependent recruitment of TFIIH modules in preinitiation complex. Molecular cell *31*, 337-346.

17. Eyboulet, F., Cibot, C., Eychenne, T., Neil, H., Alibert, O., Werner, M., and Soutourina, J. (2013). Mediator links transcription and DNA repair by facilitating Rad2/XPG recruitment. Genes Dev *27*, 2549-2562.

18. Fan, H.Y., Cheng, K.K., and Klein, H.L. (1996). Mutations in the RNA polymerase II transcription machinery suppress the hyperrecombination mutant hpr1 delta of Saccharomyces cerevisiae. Genetics 142, 749-759.

19. Felipe-Abrio, I., Lafuente-Barquero, J., García-Rubio, M.L., and Aguilera, A. (2015). RNA polymerase II contributes to preventing transcription-mediated replication fork stalls. Embo j *34*, 236-250.

20. Gaillard, H., García-Benítez, F., and Aguilera, A. (2017). Gene gating at nuclear pores prevents the formation of R loops. Mol Cell Oncol *5*, e1405140-e1405140.

21. Gallardo, M., Luna, R., Erdjument-Bromage, H., Tempst, P., and Aguilera, A. (2003). Nab2p and the Thp1p-Sac3p complex functionally interact at the interface between transcription and mRNA metabolism. The Journal of biological chemistry *278*, 24225-24232.

22. García-Benítez, F., Gaillard, H., and Aguilera, A. (2017). Physical proximity of chromatin to nuclear pores prevents harmful R loop accumulation contributing to maintain genome stability. Proceedings of the National Academy of Sciences of the United States of America *114*, 10942-10947.

23. Gardiner, F.C., Costa, R., and Ayscough, K.R. (2007). Nucleocytoplasmic trafficking is required for functioning of the adaptor protein Sla1p in endocytosis. Traffic (Copenhagen, Denmark) *8*, 347-358.

24. González-Aguilera, C., Tous, C., Gómez-González, B., Huertas, P., Luna, R., and Aguilera, A. (2008). The THP1-SAC3-SUS1-CDC31 complex works in transcription elongation-mRNA export preventing RNA-mediated genome instability. Mol Biol Cell *19*, 4310-4318.

25. González-Barrera, S., García-Rubio, M., and Aguilera, A. (2002). Transcription and double-strand breaks induce similar mitotic recombination events in Saccharomyces cerevisiae. Genetics *162*, 603-614.

26. Grünberg, S., Henikoff, S., Hahn, S., and Zentner, G.E. (2016). Mediator binding to UASs is broadly uncoupled from transcription and cooperative with TFIID recruitment to promoters. Embo j *35*, 2435-2446.

27. Guglielmi, B., Soutourina, J., Esnault, C., and Werner, M. (2007). TFIIS elongation factor and Mediator act in conjunction during transcription initiation in vivo. Proc Natl Acad Sci U S A *104*, 16062-16067.

28. Hartman, J.L.t., and Tippery, N.P. (2004). Systematic quantification of gene interactions by phenotypic array analysis. Genome Biol *5*, R49.

29. Hashimoto, S., Boissel, S., Zarhrate, M., Rio, M., Munnich, A., Egly, J.-M., and Colleaux, L. (2011). MED23 mutation links intellectual disability to dysregulation of immediate early gene expression. Science (New York, NY) *333*, 1161-1163.

30. Heberle, H., Meirelles, G.V., da Silva, F.R., Telles, G.P., and Minghim, R. (2015). InteractiVenn: a web-based tool for the analysis of sets through Venn diagrams. BMC Bioinformatics *16*, 169-169.

31. Huang, K.M., Gullberg, L., Nelson, K.K., Stefan, C.J., Blumer, K., and Lemmon, S.K. (1997). Novel functions of clathrin light chains: clathrin heavy chain trimerization is defective in light chain-deficient yeast. Journal of cell science *110 (Pt 7)*, 899-910.

32. Jeronimo, C., Langelier, M.-F., Bataille, A.R., Pascal, J.M., Pugh, B.F., and Robert, F. (2016). Tail and Kinase Modules Differently Regulate Core Mediator Recruitment and Function In Vivo. Molecular cell *64*, 455-466.

33. Jeronimo, C., and Robert, F. (2017). The Mediator Complex: At the Nexus of RNA Polymerase II Transcription. Trends Cell Biol *27*, 765-783.

34. Katou, Y., Kanoh, Y., Bando, M., Noguchi, H., Tanaka, H., Ashikari, T., Sugimoto, K., and Shirahige, K. (2003). S-phase checkpoint proteins Tof1 and Mrc1 form a stable replication-pausing complex. Nature *424*, 1078-1083.

35. Knoll, E.R., Zhu, Z.I., Sarkar, D., Landsman, D., and Morse, R.H. (2018). Role of the pre-initiation complex in Mediator recruitment and dynamics. eLife *7*, e39633.

36. Koschubs, T., Seizl, M., Larivière, L., Kurth, F., Baumli, S., Martin, D.E., and Cramer, P. (2009). Identification, structure, and functional requirement of the Mediator submodule Med7N/31. The EMBO journal *28*, 69-80.

37. Landsverk, H.B., Sandquist, L.E., Bay, L.T.E., Steurer, B., Campsteijn, C., Landsverk, O.J.B., Marteijn, J.A., Petermann, E., Trinkle-Mulcahy, L., and Syljuåsen, R.G. (2020). WDR82/PNUTS-PP1 Prevents Transcription-Replication Conflicts by Promoting RNA Polymerase II Degradation on Chromatin. Cell Rep *33*, 108469.

38. Linder, T., and Gustafsson, C.M. (2004). The Soh1/MED31 protein is an ancient component of Schizosaccharomyces pombe and Saccharomyces cerevisiae Mediator. J Biol Chem 279, 49455-49459.

39. Lisby, M., Barlow, J.H., Burgess, R.C., and Rothstein, R. (2004). Choreography of the DNA damage response: spatiotemporal relationships among checkpoint and repair proteins. Cell *118*, 699-713.

40. Liu, H., Jin, F., Liang, F., Tian, X., and Wang, Y. (2011). The Cik1/Kar3 motor complex is required for the proper kinetochore-microtubule interaction after stressful DNA replication. Genetics *187*, 397-407.

41. Liu, H., Liang, F., Jin, F., and Wang, Y. (2008). The coordination of centromere replication, spindle formation, and kinetochore-microtubule interaction in budding yeast. PLoS genetics *4*, e1000262-e1000262.

42. Love, M.I., Huber, W., and Anders, S. (2014). Moderated estimation of fold change and dispersion for RNA-seq data with DESeq2. Genome Biol *15*, 550.

43. Lydeard, J.R., Jain, S., Yamaguchi, M., and Haber, J.E. (2007). Break-induced replication and telomerase-independent telomere maintenance require Pol32. Nature *448*, 820-823.

44. Nakayashiki, T., and Mori, H. (2013). Genome-wide screening with hydroxyurea reveals a link between nonessential ribosomal proteins and reactive oxygen species production. Journal of bacteriology *195*, 1226-1235.

45. Parsons, A.B., Brost, R.L., Ding, H., Li, Z., Zhang, C., Sheikh, B., Brown, G.W., Kane, P.M., Hughes, T.R., and Boone, C. (2004). Integration of chemical-genetic and genetic interaction data links bioactive compounds to cellular target pathways. Nat Biotechnol *22*, 62-69.

46. Parsons, A.B., Lopez, A., Givoni, I.E., Williams, D.E., Gray, C.A., Porter, J., Chua, G., Sopko, R., Brost, R.L., Ho, C.H., *et al.* (2006). Exploring the mode-of-action of bioactive compounds by chemical-genetic profiling in yeast. Cell *126*, 611-625.

47. Petrenko, N., Jin, Y., Wong, K.H., and Struhl, K. (2016). Mediator Undergoes a Compositional Change during Transcriptional Activation. Molecular cell *64*, 443-454.

48. Petrenko, N., Jin, Y., Wong, K.H., and Struhl, K. (2017). Evidence that Mediator is essential for Pol II transcription, but is not a required component of the preinitiation complex in vivo. eLife *6*, e28447.

49. Plaschka, C., Lariviere, L., Wenzeck, L., Seizl, M., Hemann, M., Tegunov, D., Petrotchenko, E.V., Borchers, C.H., Baumeister, W., Herzog, F., *et al.* (2015). Architecture of the RNA polymerase II-Mediator core initiation complex. Nature *518*, 376-380.

50. Poli, J., Gasser, S.M., and Papamichos-Chronakis, M. (2017). The INO80 remodeller in transcription, replication and repair. Philos Trans R Soc Lond B Biol Sci *372*.

51. Poli, J., Gerhold, C.-B., Tosi, A., Hustedt, N., Seeber, A., Sack, R., Herzog, F., Pasero, P., Shimada, K., Hopfner, K.-P., *et al.* (2016). Mec1, INO80, and the PAF1 complex cooperate to limit transcription replication conflicts through RNAPII removal during replication stress. Genes & development *30*, 337-354.

52. Prado, F., and Aguilera, A. (2005). Impairment of replication fork progression mediates RNA polII transcription-associated recombination. Embo j *24*, 1267-1276.

53. Promonet, A., Padioleau, I., Liu, Y., Sanz, L., Biernacka, A., Schmitz, A.L., Skrzypczak, M., Sarrazin, A., Mettling, C., Rowicka, M., *et al.* (2020). Topoisomerase 1 prevents replication stress at R-loop-enriched transcription termination sites. Nat Commun *11*, 3940.

54. Ramírez, F., Ryan, D.P., Grüning, B., Bhardwaj, V., Kilpert, F., Richter, A.S., Heyne, S., Dündar, F., and Manke, T. (2016). deepTools2: a next generation web server for deep-sequencing data analysis. Nucleic acids research *44*, W160-W165.

55. Risheg, H., Graham, J.M., Jr., Clark, R.D., Rogers, R.C., Opitz, J.M., Moeschler, J.B., Peiffer, A.P., May, M., Joseph, S.M., Jones, J.R., *et al.* (2007). A recurrent mutation in MED12 leading to R961W causes Opitz-Kaveggia syndrome. Nature genetics *39*, 451-453.

56. Rouse, J., and Jackson, S.P. (2002). Lcd1p recruits Mec1p to DNA lesions in vitro and in vivo. Molecular cell *9*, 857-869.

57. Santocanale, C., and Diffley, J.F. (1998). A Mec1- and Rad53-dependent checkpoint controls late-firing origins of DNA replication. Nature *395*, 615-618.

58. Santos-Pereira, J.M., and Aguilera, A. (2015). R loops: new modulators of genome dynamics and function. Nature reviews Genetics *16*, 583-597.

59. Santos-Rosa, H., Clever, B., Heyer, W.D., and Aguilera, A. (1996). The yeast HRS1 gene encodes a polyglutamine-rich nuclear protein required for spontaneous and hpr1-induced deletions between direct repeats. Genetics *142*, 705-716.

60. Schneider, M., Hellerschmied, D., Schubert, T., Amlacher, S., Vinayachandran, V., Reja, R., Pugh, B.F., Clausen, T., and Köhler, A. (2015). The Nuclear Pore-Associated TREX-2 Complex Employs Mediator to Regulate Gene Expression. Cell *162*, 1016-1028.

61. Sogo, J.M., Lopes, M., and Foiani, M. (2002). Fork reversal and ssDNA accumulation at stalled replication forks owing to checkpoint defects. Science *297*, 599-602.

62. Soutourina, J. (2018). Transcription regulation by the Mediator complex. Nat Rev Mol Cell Biol *19*, 262-274.

63. Syring, I., Klümper, N., Offermann, A., Braun, M., Deng, M., Boehm, D., Queisser, A., von Mässenhausen, A., Brägelmann, J., Vogel, W.*, et al.* (2016). Comprehensive analysis of the transcriptional profile of the Mediator complex across human cancer types. Oncotarget *7*, 23043-23055.

64. Tercero, J.A., and Diffley, J.F. (2001). Regulation of DNA replication fork progression through damaged DNA by the Mec1/Rad53 checkpoint. Nature *412*, 553-557.

65. Tong, A.H., and Boone, C. (2006). Synthetic genetic array analysis in Saccharomyces cerevisiae. Methods Mol Biol *313*, 171-192.

66. Tsai, K.-L., Yu, X., Gopalan, S., Chao, T.-C., Zhang, Y., Florens, L., Washburn, M.P., Murakami, K., Conaway, R.C., Conaway, J.W.*, et al.* (2017). Mediator structure and rearrangements required for holoenzyme formation. Nature *544*, 196-201.

67. Usui, T., and Petrini, J.H.J. (2007). The Saccharomyces cerevisiae 14-3-3 proteins Bmh1 and Bmh2 directly influence the DNA damage-dependent functions of Rad53. Proceedings of the National Academy of Sciences of the United States of America *104*, 2797-2802.

68. Woolstencroft, R.N., Beilharz, T.H., Cook, M.A., Preiss, T., Durocher, D., and Tyers, M. (2006). Ccr4 contributes to tolerance of replication stress through control of CRT1 mRNA poly(A) tail length. Journal of cell science *119*, 5178-5192.

69. Zeman, M.K., and Cimprich, K.A. (2014). Causes and consequences of replication stress. Nat Cell Biol *16*, 2-9.

70. Zettel, M.F., Garza, L.R., Cass, A.M., Myhre, R.A., Haizlip, L.A., Osadebe, S.N., Sudimack, D.W., Pathak, R., Stone, T.L., and Polymenis, M. (2003). The budding index of Saccharomyces cerevisiae deletion strains identifies genes important for cell cycle progression. FEMS Microbiol Lett *223*, 253-258.

71. Zhang, Y., Liu, T., Meyer, C.A., Eeckhoute, J., Johnson, D.S., Bernstein, B.E., Nusbaum, C., Myers, R.M., Brown, M., Li, W.*, et al.* (2008). Model-based Analysis of ChIP-Seq (MACS). Genome Biology *9*, R137.

72. Zhou, C., Elia, A.E.H., Naylor, M.L., Dephoure, N., Ballif, B.A., Goel, G., Xu, Q., Ng, A., Chou, D.M., Xavier, R.J.*, et al.* (2016). Profiling DNA damage-induced phosphorylation in budding yeast reveals diverse signaling networks. Proceedings of the National Academy of Sciences of the United States of America *113*, E3667-E3675.

73. Zou, L., and Elledge, S.J. (2003). Sensing DNA damage through ATRIP recognition of RPA-ssDNA complexes. Science (New York, NY) *300*, 1542-1548.

Table 1 - Yeast strains

Name	Genotype	Reference
yHA-1053	*MAT*a his3del1 leu2del0 lys2+ met15del0 ura3del0 (BY4742) *DDC2-yEGFP::CaURA3, can1::STE2pr-SpHIS5, lyp1::STE3pr-LEU2*	This study
yHA-269 Pol ε-MYC	*MAT*a *ade2-1 trp1-1 his3-11 his3-15 ura3-1 leu2-3 leu2-112 RAD5-(W303)* *POL E-9xMYC::KanMX bar1Δ::NatMX*	This study
yHA-1119 *soh1Δ*	Isogenic to yHA-269 except *soh1Δ::TRP*	This study
yHA-1120 *srb2Δ*	Isogenic to yHA-269 except *srb2Δ::TRP*	This study
yHA-1143 Soh1-myc	*MAT*a *ade2-1 trp1-1 his3-11 his3-15 ura3-1 leu2-3 leu2-112 RAD5+ (W303)* *pep4::LEU2 bar1Δ::NAT SOH1-13Myc::HIS*	This study
yHA-265	*MAT*a ade2-1 trp1-1 his3-11 his3-15 ura3-1 leu2-3 leu2-112 *RAD5*+ (W303) *bar1Δ::LEU2 DDC2-YFP*	(Lisby et al., 2004)
yHA-1214 *soh1Δ*	Isogenic to yHA-265 except *soh1Δ::HpH*	This study
yHA-1215 *srb2Δ*	Isogenic to yHA-265 except *srb2Δ::HpH*	This study
yHA-1259 *soh1Δ*	*MAT*a ade2-1 trp1-1 his3-11 his3-15 ura3-1 leu2-3 leu2-112 *RAD5*+ (W303) *bar1Δ::NatMX DDC2-YFP soh1Δ::HpH*	This study
yHA-1260 *srb2Δ*	*MAT*a ade2-1 trp1-1 his3-11 his3-15 ura3-1 leu2-3 leu2-112 *RAD5*+ (W303) *bar1Δ::NatMX DDC2-YFP srb2Δ::HpH*	This study

Table 2 – qPCR Primers

Target	Sequence
ARS607 ChIP-qPCR F	CTTTAGCTGGGTTTATGGGAGGTT
ARS607 ChIP-qPCR R	TAATGCACGAGCCGAAACAA
ARS607+1kb ChIP-qPCR F	GGAGAGAATCTTACCTCAGAGTGC
ARS607+1kb ChIP-qPCR R	GGGATCTTGAAAGTAAAACAGGTG
ARS607+2kb ChIP-qPCR F	CGCAGCAGTGGAGTTATCAG
ARS607+2kb ChIP-qPCR R	TAATCCACTTTGTCGGGCCA
ARS607+3kb ChIP-qPCR F	CTTTGTTATGGACCCGGAGA
ARS607+3kb ChIP-qPCR R	CATCAAGATGGAATACTGTGACAA
ARS607+4kb ChIP-qPCR F	TATGCTATCGTCGAGATGTTGTTCT
ARS607+4kb ChIP-qPCR R	GGTGGAAGCGCAGGTTGATC
ARS607+6kb ChIP-qPCR F	GTTTCACCTCGTAGTCCCTCA
ARS607+6kb ChIP-qPCR R	AACCAAATGCATTGCTTTATCA
ARS607+14kb ChIP-qPCR F	CAGGATATGCGGCCAAATTT
ARS607+14kb ChIP-qPCR R	GCATGACAGCCGAATCGAT
ARS501 ChIP-qPCR F	AAGCAAATTGCAGAAGGTTATGAA
ARS501 ChIP-qPCR R	TTCAAGGCTCTAGCATATGAAACG
EFB1 ChIP-qPCR F	GTTCAACCACATCGCTTCC
EFB1 ChIP-qPCR R	AGCCTTCAACTTTTCAGCTTC
GLY1 ChIP-qPCR F	GCACACAAACGCAAACATAAAC
GLY1 ChIP-qPCR R	CCCAGAGACACAGAACAAAC
HSP150 ChIP-qPCR F	CAACCAATCTCCACTACATCC
HSP150 ChIP-qPCR R	ACCATCACCAATTTGAGAGAC
SPF1 DRIP-qPCR F	CCCGTGGTAAACCTTTAGAAA
SPF1 DRIP-qPCR R	ATATGAACGGCAAATTGAGAC
GCN4 DRIP-qPCR F	TTGTGCCCGAATCCAGTGA
GCN4 DRIP-qPCR R	TGGCGGCTTCAGTGTTTCTA
PDC1 DRIP-qPCR F	CCTTGATACGAGCGTAACCATCA
PDC1 DRIP-qPCR R	GAAGGTATGAGATGGGCTGGTAA
PDR5 DRIP-qPCR F	TACGTCTTGTTTCGGCCTTAATC
PDR5 DRIP-qPCR R	GTCAGAGGCTATATTTCACTGGAGAA

SUPPLEMENTARY FIGURES AND LEGENDS

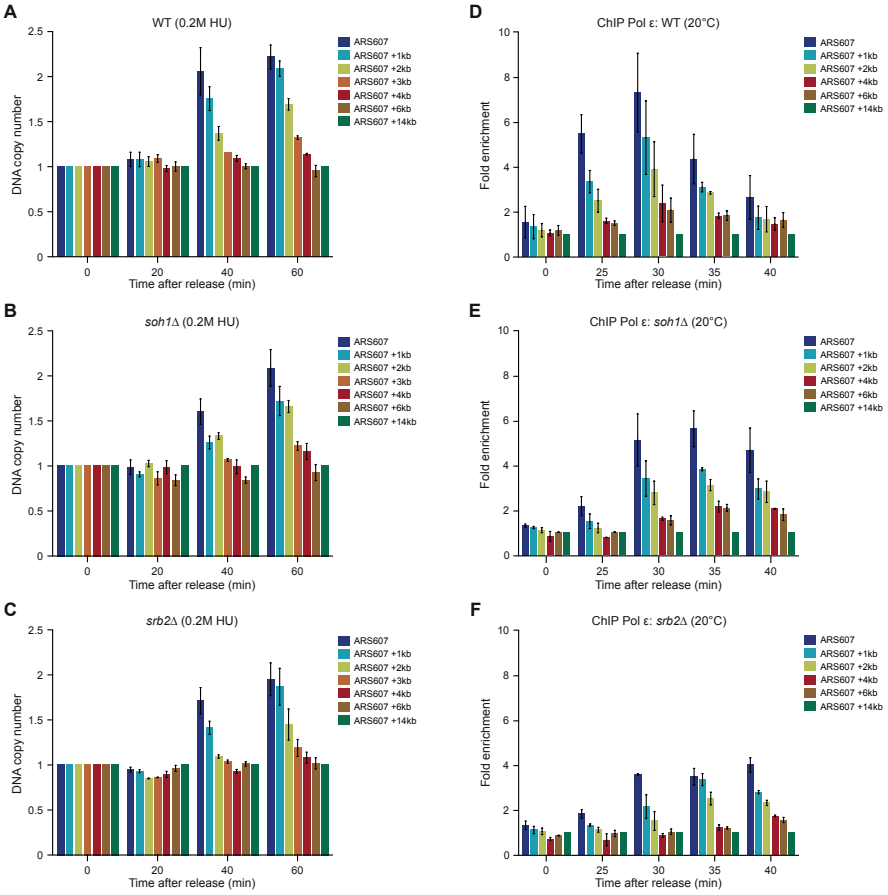

S1 Figure. Copy number assays and unstressed replication fork progression *soh1Δ* and *srb2Δ* mutants. Copy number assays of (A) WT, (B) *soh1Δ* and (C) *srb2Δ* strains at ARS607. Data are represented as the mean fold change from three independent experiments ± s.e.m. ChIP-qPCR assay of Pol ε of (D) WT, (E) *soh1Δ* and (F) *srb2Δ* strains at ARS607 at 20ºC (unstressed conditions). Data are represented as the mean fold change from three independent experiments ± s.e.m.

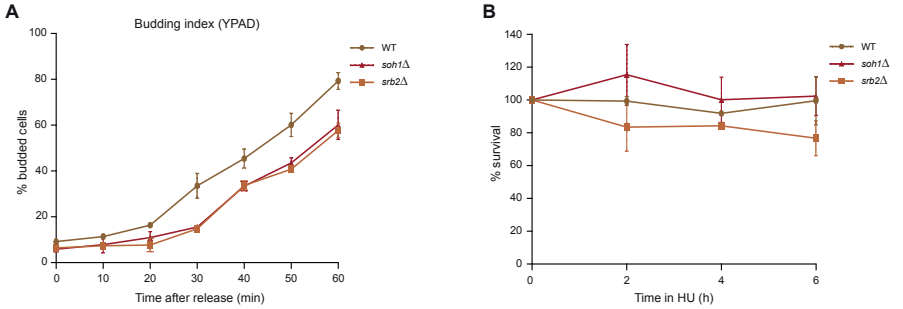

S2 Figure. Budding index and survival assays of *soh1Δ* and *srb2Δ* mutants.
(A) Budding index for WT, *soh1Δ* and *srb2Δ* strains arrested in G1-phase and released in S-phase in unstressed conditions. Data are represented from three independent experiments ± s.e.m. (D) Survival assay of WT, *soh1Δ* and *srb2Δ* strains after exposure to HU for the indicated time periods. Data are represented from three independent experiments ± s.e.m.

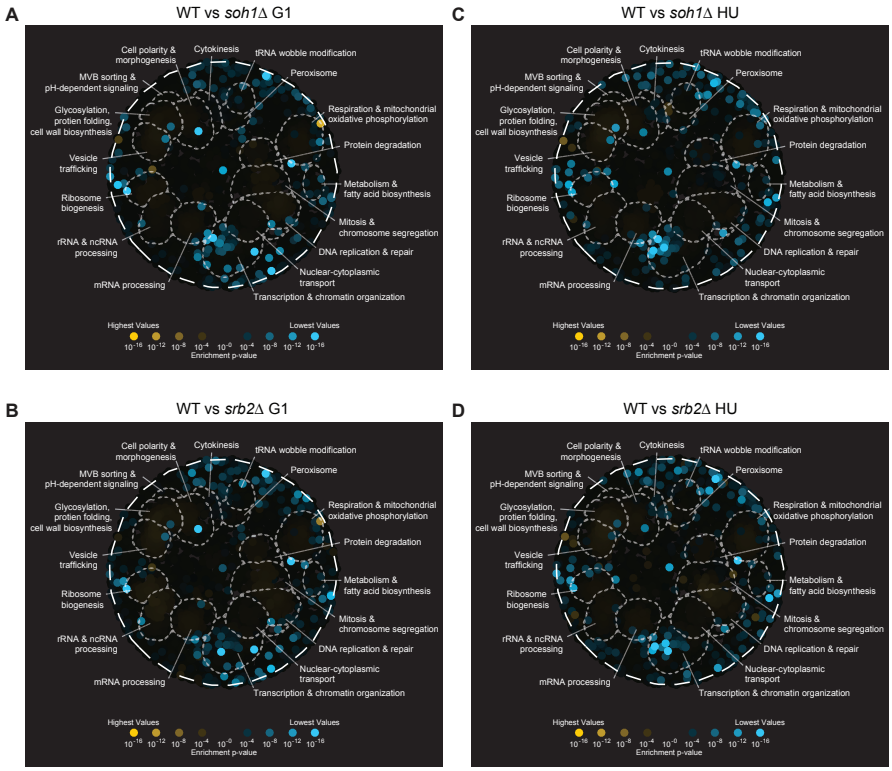

S3 Figure. SAFE analysis of transcriptome changes in Mediator mutants.
SAFE analysis depicts enrichment of the RNA-seq data in functional domains based on genetic interaction and GO enrichment data for (A) *soh1Δ* in G1-phase, (B) *srb2Δ* in G1-phase, (C) *soh1Δ* in S-phase with HU and (D) *srb2Δ* in S-phase with HU.

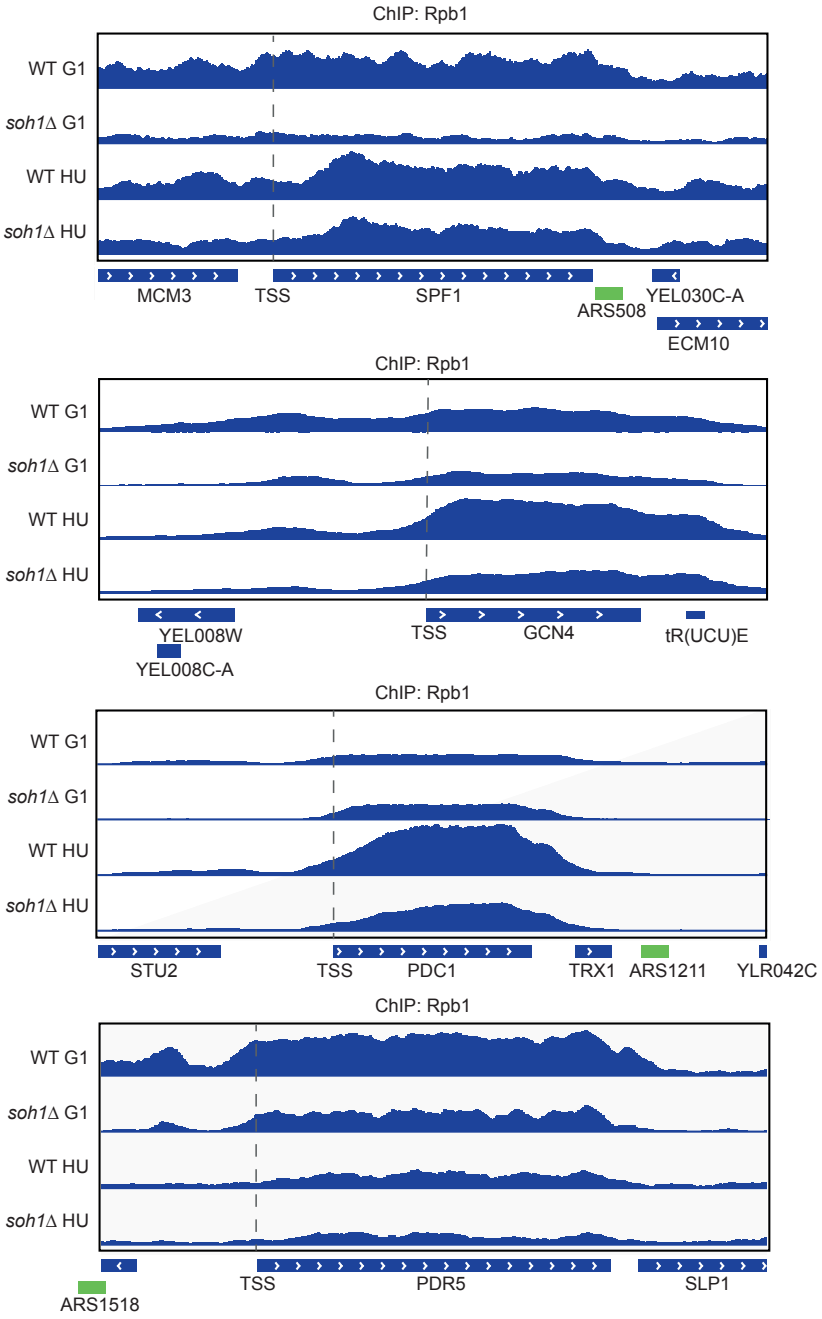

S4 Figure. RNAPII signal across the *SPF1*, *GCN4*, *PDC1* and *PDR5* genes in WT and *soh1Δ* and *srb2Δ* mutants in G1-phase and S-phase with HU.